

Influence of Non-Conductive Probes on Specific Absorption Rate

S. Oh¹, and C. M. Collins¹

¹PSU College of Medicine, Hershey, PA, United States

Introduction:

An increasing number of interventional studies are being developed in which minimally invasive procedures are performed using MRI guidance [1]. Thin and precisely controlled devices, guided wires, and sensors facilitate these during MR scanning. While several studies have reported the MR safety-related issues of metallic devices and wires [2-4], the influences of non-conductive devices on the specific absorption rate (SAR) of surrounding tissues are rarely investigated. In this study, we show that even non-conductive probes, e.g., fiber optic thermal/pressure sensors, catheters, etc., can affect SAR.

Methods:

We modeled fiber optic thermal probes (OPT-M, opSens, Canada) inserted into a conductive phantom within a 12-rung head size birdcage RF coil using the Finite-Difference Time-Domain (FDTD) method with commercially-available software (xFDTD; Remcom, Inc.) as shown in Figure 1. The thermal probe (cable and probe tip) is non-conductive and has low relative-permittivity (ϵ_r) as shown in Table 1. The diameter of probe tip and cable were 1.2 mm and 1.0 mm, respectively, but were modeled as 2 mm due to the cell size. The cell and mesh size of the FDTD model were $2 \times 2 \times 2 \text{ mm}^3$ and $240 \times 240 \times 280$, respectively. 50-ohm terminated current sources and the Liao outer boundary condition [5] were used. Two fiber optic probes were placed in the conductive phantom (height \times width \times length= $64 \times 92 \times 156 \text{ mm}^3$) at the central-axial plane ($z=0 \text{ mm}$), as in Figure 1(b) and (c). Each probe was located at different depths, one was at the center and the other was close to surface, as in Figure 1(b). Probes, phantom, and RF coil are modeled to match experiments in our laboratory. The case without probes was also simulated. Dissipated power in the phantom of two different FDTD simulations (with and without probes) were scaled to 5.25W. Current density and electric field data were recorded. The SAR distribution on the central-axial plane was calculated using equation (1), where J , E , ρ are current density, electric field, and material density, respectively, at position x , y , and z .

$$\text{SAR} = \frac{J_x E_x}{2\rho_x} + \frac{J_y E_y}{2\rho_y} + \frac{J_z E_z}{2\rho_z} \quad (1)$$

Results and Conclusion:

RF-induced eddy currents are forced to flow around non-conductive objects and tissues, resulting in regions of locally high SAR adjacent the non-conducting surfaces. Figure 2(b) shows typical SAR distribution when RF power is applied to a conductive phantom [6]. The SAR increases with distance from the center, in agreement with electromagnetic theory and experiment [6]. A significant increase in SAR is observed around the fiber optic thermal probes even though the probes are all non-conductive materials, as seen in Table 1 and Figure 2(a). The probe near the surface shows greater absolute increase in SAR, since it is in the region of higher current density. The difference between the two SAR maps is shown in Figure 2(c), and one dimensional profiles, Figure 2(d), clearly show the non-conductive probes have effects on SAR, with increases in one-cell SAR in excess of 100% of the case with no probes. While this may be orders of magnitude smaller than increases achievable with conductive probes, it is worth considering in attempts to measure temperature with fiber optic probes and in assessments of RF safety.

Acknowledgment: This study was funded by NIH R01 EB000454.

References:

- [1] Bock *et al.*, J. Magn Reson Imaging 2008;27:326-338
 [2] Shellock *et al.*, New York: Raven Press, 1994
 [3] Shellock *et al.*, J Magn Reson Imaging 1996;6:271-272
 [4] Konings *et al.*, J Magn Reson Imaging 2000;12:79-85
 [5] Liao, Scientia Sinica 1984;27A:1063-76
 [6] Oh *et al.*, Magn Reson Med in press

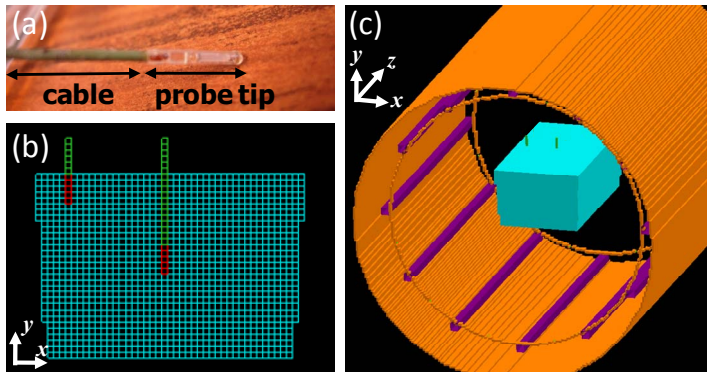


Table 1. Dielectric properties

| | σ [S/m] | ϵ_r | ρ [kg/m ³] |
|-------------------|----------------|--------------|-----------------------------|
| Phantom | 1.895 | 77.99 | 1050 |
| Probe tip (glass) | 0 | 4.7 | 2600 |
| Cable (Teflon) | 0 | 2.1 | 2200 |

Figure 1 (a) Fiber optic thermal probe. (b) Location of probes in the conductive phantom. Red, green, and light blue indicate probe tip, cable, and phantom, respectively. (c) The phantom located at the center of the 12-rung head size birdcage RF coil.

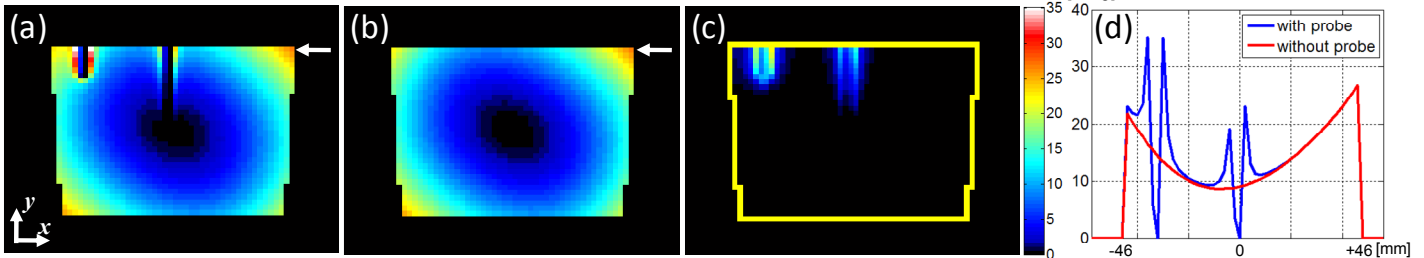


Figure 2. (a) SAR map at the center of the phantom with the fiber optic probes, (b) without probes, and (c) difference of two SAR maps. Yellow line indicates the boundary of the phantom. Three SAR maps are all expressed in the same color scale with units of W/kg. (d) SAR distribution along the top surface of the phantom on the plane shown in (a) and (b), as indicated by white arrows.